



AGING BEHAVIOR IN CO-CR-MO-C ALLOYS

Alfirano, Anistasia Milandia and Suryana

Metallurgical Engineering Department, Sultan Ageng Tirtayasa University, Cilegon, Indonesia

E-Mail: alfirano@ft-untirta.ac.id

ABSTRACT

The effects of the addition of 1 wt. % Si and 1 wt. % Mn in Co-28Cr-6Mo-0.25C alloys on phase of precipitate during aging at 873–1473 K have been investigated. The precipitation in the Cobalt matrix was observed in the aged specimens. The result shows that the precipitation consists of fine precipitation of $M_{23}C_6$ type, η -phase and σ -phase. Meanwhile, the addition of Si increased the precipitation area in the Time-Temperature-Precipitation (TTP) diagram as compared to the Mn. The addition of Si increased the precipitation area of η -phase. During aging, precipitate size decreased with decreasing aging temperature. Blocky and rod-like precipitates were observed at higher and lower aging temperatures, respectively. The addition of Si increased the hardness of alloy that might be caused by the formation of fine $M_{23}C_6$ type and η -phase precipitates at 1073-1173 K.

Keywords: co-Cr-Mo, aging, Si, Mn, precipitate, TTP diagram, hardness.

INTRODUCTION

Co-Cr-Mo implant alloys are currently applied as primary materials for orthopedic implant because of their excellent wear and corrosion resistance. The main strengthening mechanism of this alloy is the presence of second phase precipitate. The precipitate shows in the alloys are closely related to the phase, size, amount, and distribution of precipitates in the metallic matrix [1, 2]. Aging treatment in Co-Cr-Mo alloys contributes to the formation of various microstructural features including precipitation of precipitates which can affect the properties of the alloy [3, 4]. Montero et al. have shown that isothermal aging of Co-27Cr-5Mo-0.05C alloy at 1073 K significantly improved the corrosion resistance [3].

In view point of microstructure of aged-alloys, Rajan and Van der Sande [5] shows that intrinsic stacking faults, known as intragranular striations was the preferential sites for precipitation. They reported that aging promotes the formation of stacking faults as well as a martensitic transformation from fcc to a heavily faulted hcp phase. For aging between 923 K and 1423 K, Taylor and Waterhouse reported the formation of $M_{23}C_6$ carbide at intragranular striations as a preferential site for precipitation [4]. Lane and Grant proposed that aging not only caused the precipitation of Cr_4C but also converted the Cr_7C_3 to Cr_4C [6]. After aging in Hastelloy X, the precipitate such as $M_{23}C_6$ and σ -phase were observed at temperature up to 1173 K from TTP diagram constructed by Zhao *et al* [7]. The effects of Si and Mn on the phase and dissolution behaviors of precipitates during solution treatment have been clarified [8, 9, 10]. Precipitates detected in Co-28Cr-6Mo-0.25C-1Si-1Mn alloys (mass%) during solution treatment were $M_{23}C_6$ type, η -phase (M_6C - $M_{12}C$ type), π -phase (M_2T_3X type with β -Mn structure), and χ -phase (α -Mn structure). Furthermore, the objective of this study is to investigate the effect of Si and Mn on the phase and formation of the precipitates in ASTM F75

Co-Cr-Mo alloys during aging, based on the observation of microstructure of aged Co-Cr-Mo-C-Si-Mn alloys.

METHODS

CCM alloy ingots were prepared by vacuum furnace melting and cast in a copper mold. The chemical compositions of the ingots are listed in Table-1. Co-28Cr-6Mo-0.25C alloys with 1 mass% Si, 1 mass% Mn and 1 mass% Si, Mn are referred to as CCM1, CCM2 and CCM3, respectively. The alloys were solution-treated at temperatures of 1548 K for a holding time of 43.2 ks. The alloys were water-quenched immediately after heat treatment.

Table-1. Chemical compositions of alloys (wt.%).

Notation	Cr	Mo	C	Si	Mn	Co
CCM1	29.17	6.22	0.23	0.96	0.08	Bal.
CCM2	27.86	6.03	0.25	0.11	0.97	Bal.
CCM2	27.96	6.09	0.26	0.98	1.02	Bal.

carbide dissolution was achieved during solution treatment. Aging was carried out at 873–1473 K for 0.6–43.8 ks. The specimen surfaces were mechanically ground with emery papers up to #1500 and polished with a diamond paste having a grain size of 0.1 μ m. The specimens were electrolytically etched in 10% H_2SO_4 -methanol solution at 6 V for microstructural observation. The microstructure of the alloys was observed using an optical microscope and a scanning electron microscope. Precipitates in the as-cast and heat-treated alloys were electrolytically extracted in 10% H_2SO_4 aqueous solution at 2 V. The phase and morphology of the extracted precipitates were identified using X-ray diffraction and SEM, respectively.



RESULTS AND DISCUSSIONS

In the aging treatment, those as-cast specimens were solution-treated at 1523 K for 43.2 ks until complete precipitates dissolution was achieved. From XRD analysis as shown in Figure-1, only γ and ϵ -phases were detected after solution treatment.

Previous reports have been shown that quenching the Co-Cr-Mo alloy promotes the formation of ϵ -martensite [11]. The microstructures CCM1 alloy during aging at 1073 K to 1373 K for 43.8 ks is illustrated in Figure-2. As can be seen in these figures, aging at 1073 K caused the progressive formation of very fine precipitates along intra-granular striation and the matrix. Intra-granular striations were clearly visible at the precipitation sites within a relatively large density of stacking faults. At 1373

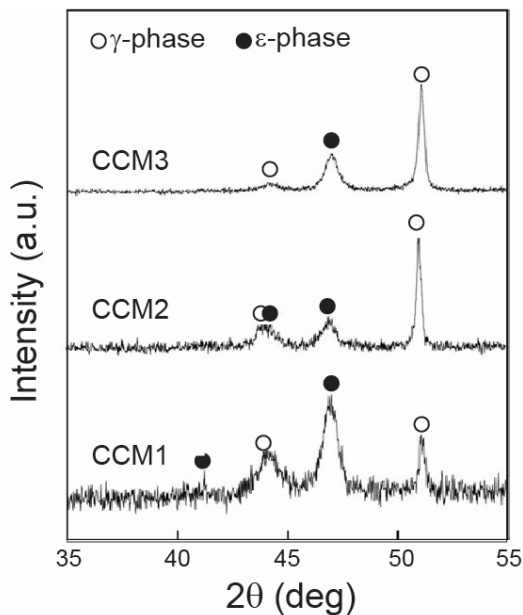


Figure-1. XRD patterns of solution-treated alloys.

K, σ -phase was mainly formed on grain boundary. Figure-3 illustrates the microstructures of the alloys aged at 1073 K, 1173 K, 1273 K and 1373 K for 43.8 ks. Different precipitate morphologies are associated with the aging temperature. At low temperature of experiment, rod-like precipitate was observed in all alloys. With increasing aging temperature, the precipitate size was increased and it seems to be a blocky-densed shape.

RESULTS AND DISCUSSIONS

In the aging treatment, those as-cast specimens were solution-treated at 1523 K for 43.2 ks until complete precipitates dissolution was achieved. From XRD analysis as shown in Figure-1, only γ and ϵ -phases were detected after solution treatment.

Previous reports have been shown that quenching the Co-Cr-Mo alloy promotes the formation of ϵ -martensite [11]. The microstructures CCM1 alloy during aging at 1073 K to 1373 K for 43.8 ks is illustrated in Figure-2. As can be seen in these figures, aging at 1073 K caused the progressive formation of very fine precipitates along intra-granular striation and the matrix. Intra-granular striations were clearly visible at the precipitation sites within a relatively large density of stacking faults. At 1373 K, σ -phase was mainly formed on grain boundary. Figure-3 illustrates the microstructures of the alloys aged at 1073 K, 1173 K, 1273 K and 1373 K for 43.8 ks. Different precipitate morphologies are associated with the aging temperature. At low temperature of experiment, rod-like precipitate was observed in all alloys. With increasing aging temperature, the precipitate size was increased and it seems to be a blocky-densed shape.

Using XRD analyzer, the phases formed during aging from 1073 K to 1373 K in CCM1, CCM2 and CCM3 alloys have been examined. Figure-4 shows XRD pattern of CCM1 alloy aged at 1373 K with various aging time. $M_{23}C_6$ was the main phase at short heating time. For longer heating time, $M_{23}C_6$ was gradually transformed into σ -phase, as this phase to be a main phase at 43.2 ks. In the alloy containing Mn, σ -phase was not formed. It implies that Si addition accelerates σ -phase precipitation, mainly in grain boundary. In stainless steel system, $M_{23}C_6$ will be as a nucleation sites for σ -phase [12].

The results of XRD analysis for all alloys have been used to build time-temperature-precipitation (TTP) diagram which described completely in Figure-5. An $M_{23}C_6$ -type is a main precipitate in all alloys. Meanwhile, η -phase was detected in all alloys at the temperature range of 1173 K to 1273 K. The η -phase and σ -phase were observed in the lower and upper temperature ranges, respectively, in the TTP diagram of CCM1 alloy. The nose of the TTP diagram for $M_{23}C_6$ type precipitation occur at about 1200 K for less than 2.4 ks in Si contained alloys and at about 1173 K for less than 2,4 ks in Mn contained alloy. The nose of the TTP diagram for η -phase precipitation was occurred at about 1180 K for less than 2.4 ks in Si-contained alloys and at about 1170 K for less than 22 ks in Mn-contained alloy. From the figures, we can infer that the addition of Mn decreased the precipitation area of all the precipitate phases in the TTP diagram, which was not the case with the addition of Si.

Aging also has the effect on increasing the hardness of the alloys. Figure-6 shows the hardness of solution-treated and aged CCM1, CCM2 and CCM3 alloys at the different aging temperature for heating time of 43.2 ks. The hardness of aged alloys is higher compared to that of solution-treated alloys. At aging temperature up to 1173 K, the hardness of all aged alloys was increased. Furthermore, the hardness will be gradually decreased for

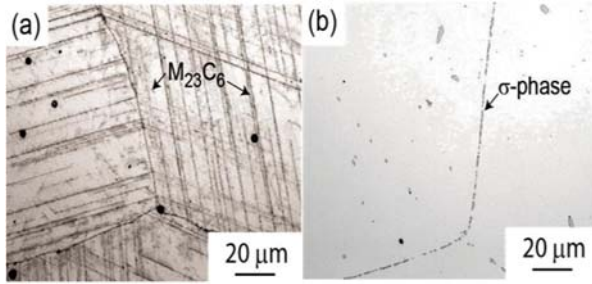


Figure-2. Microstructure of CCM1 alloy aged at (a) 1073 K and (b) 1373 K for 43.2 ks.

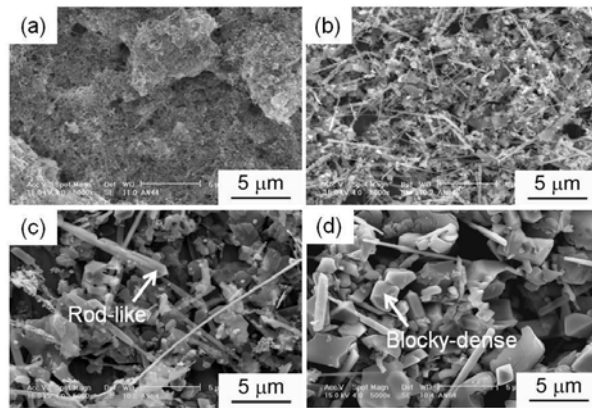


Figure-3. Morphology of precipitates formed in CCM3 alloy aged at 1073 K–1373 K for 43.8 ks.

aging temperature more than 1173 K.

Aging at 1073 K and 1173 K produced a fine precipitate in CCM1, CCM2 and CCM3 alloys. The

precipitation was took place in the interior of grain on the dislocations and the stacking faults [4]. After solution treatment, microstructure exhibited long stacking faults coupled with intragranular striations. These striations became clearly seen after precipitation occurred. The random dispersion of fine precipitates on the stacking faults might be due to the solute Suzuki segregation mechanism as a mode of nucleation for precipitation due

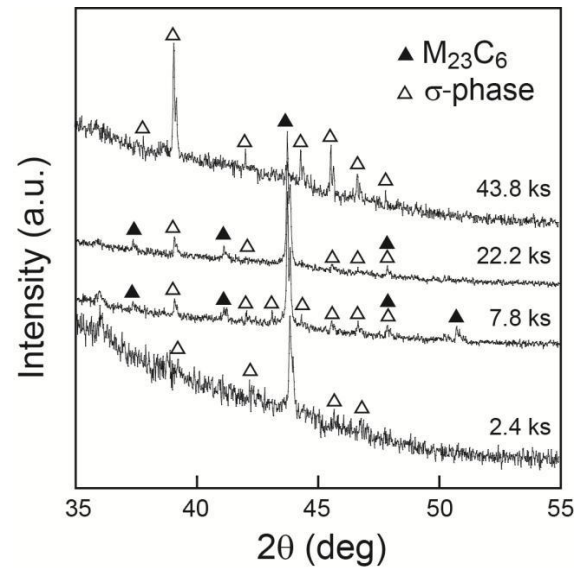


Figure-4. XRD pattern of aged CCM1 alloys at 1373 K.

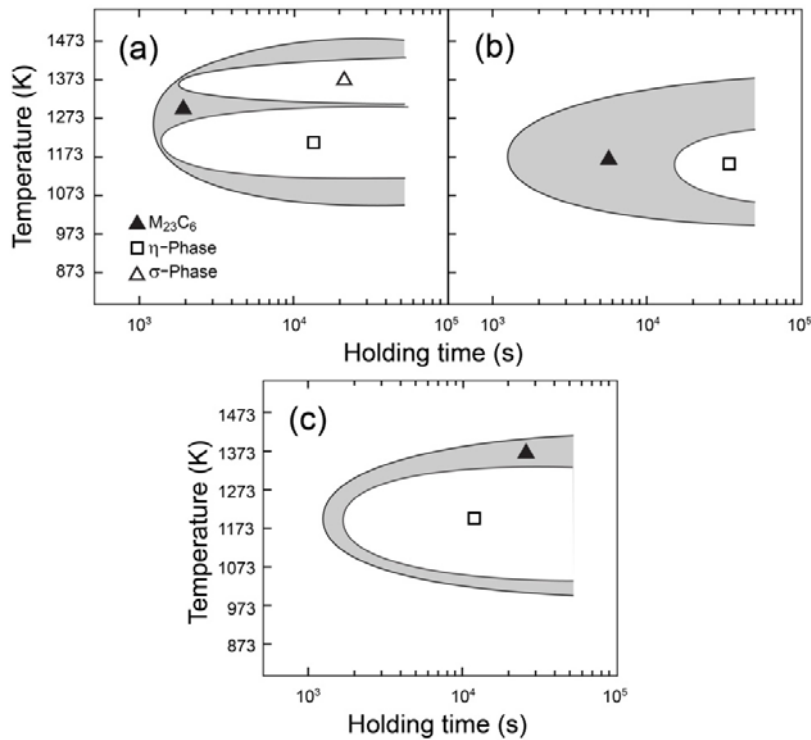


Figure-5. Time-temperature-precipitation diagrams of (a) CCM1, (b) CCM2 and (c) CCM3 alloys.

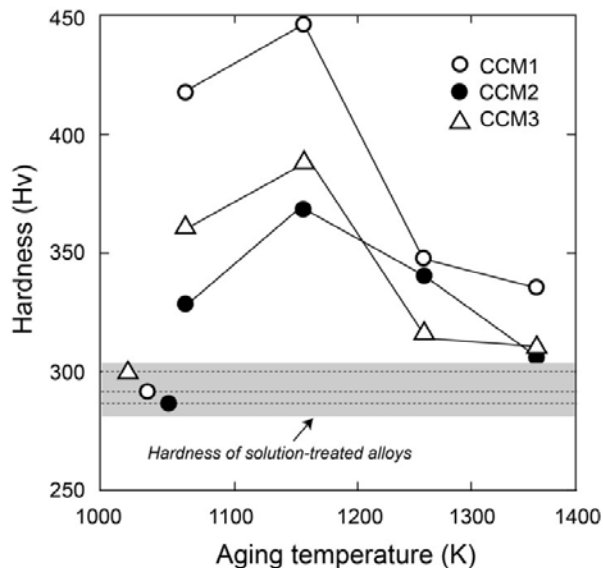


Figure-6. Hardness of alloys for aging time of 43.2 ks.

of carbon [4]. However, as is well known, carbon atoms have a tendency to be attracted to dislocations and stacking faults and form carbon segregation zones. It was the carbon segregation promoted the nucleation and the subsequent growth on the faulted regions. This carbon atom might be reacts with solute Cr and Mo which also

diffuse preferentially at dislocations and stacking faults [4]. In Co-Cr-Mo-C alloys, the $M_{23}C_6$ type precipitate has a complex fcc structure. The possible mismatch between cobalt matrix and this precipitate showed that the fcc cobalt {111} and hcp cobalt {0001} planes were identical in both atomic spacing and arrangement [4]. Therefore the $M_{23}C_6$ type {111} planes would be matched when precipitating on intrinsic stacking faults of the matrix.

Besides the $M_{23}C_6$ type precipitate, η -phase was detected as a minor precipitate during aging. In the Co-Cr-Mo-Ni system, Kurosu *et al.* reported the formation of intermetallic σ -phase during aging, which took place in the grain boundary [13]. Since the carbon content of the alloys used in this study was 0.25mass%, the σ -phase formation was not detected. The possible mechanism is that the σ phase might react with the solute carbon to form $M_{23}C_6$ -type and η -phase precipitates. The formation of η -phase was detected both in the alloys with and without Si addition. From TTP diagrams, precipitation area of η -phase in the alloy containing Si is larger compared to that of the alloy containing Mn. It is also found that η -phase precipitation in Si-contained alloys is much faster than in Mn-contained alloy. It was suggested that Si enhances the formation of η -phase in Co-Cr-Mo-C alloys, resulted the bigger TTP diagram area in the Si contained alloys compared to that of Mn contained alloy.

The preferential sites for precipitation affect the morphology of precipitate formed during aging [4]. Two



types of mechanisms were found which related to the formation of precipitate morphology in Co-Cr-Mo alloys. At low temperatures (below 1200 K), the precipitation occurred on the stacking faults probably by means of Suzuki segregation mechanism. Furthermore, the precipitates that nucleated on the stacking faults grew into fine precipitate with lath/rod-like shape. Meanwhile, at higher temperatures (above 1200 K), the precipitation of carbides occurred on the dislocation defect. In this condition, blocky dense precipitate was observed as a result of precipitate spheroidization and growth takes place along plane of {111} type [8].

Micro hardness test was carried out to the aged alloys. From the results, it was apparent that aging temperature has the effect on the hardness of alloys. The highest hardness value was achieved in the aging temperature of 1173 K. In this condition, fine precipitates of $M_{23}C_6$ and η -phase dispersed along the stacking faults might be has responsibility on increasing in hardness values. In contrast the precipitates formed in the dislocation at higher temperatures had only minimal effect on the alloys hardness. It was suggested that that both the precipitate and the stacking fault contributed to the strengthening [4].

CONCLUSIONS

The effects of the addition of 1 wt. % Si and 1 wt. % Mn in Co-28Cr-6Mo-0.25C alloys on aging behavior at 873-1473 K have been investigated. Si and Mn affected the phase of precipitates formed during aging. $M_{23}C_6$, η -phase and σ -phase were observed in the aged CCM1, CCM2 and CCM3 alloys. η -phase precipitation in Si contained alloys is faster than in Mn contained alloy. Precipitate size decreased with decreasing aging temperature. Blocky and rod-like precipitates were observed at higher and lower aging temperatures, respectively. The addition of Si increased the hardness due to the formation of fine $M_{23}C_6$ and η -phase precipitates at 1073-1173 K which dispersed along the stacking faults.

REFERENCES

- [1] Morral F. R. 1966. Cobalt alloys as implants in humans. *J. Mater.* 1: 384-412.
- [2] Noble P.C. 1983. Special materials for the replacement of human joints. *Met. Forum.* 6: 59-80.
- [3] C. Montero-Ocampo, M. Talavera, and H. Lopez. 1999. Effect of alloy preheating on the mechanical properties of as-cast Co-Cr-Mo-C alloys. *Metall. Mater. Trans. A.* 30A: 611-620.
- [4] R.N.J. Taylor and R.B. Waterhouse. 1983. A study of the ageing behaviour of a cobalt based implant alloy. *J. Mater. Sci.* 18: 3265-3280.
- [5] K. Rajan and J.D. Vander Sande. 1982. Room temperature strengthening mechanisms in a Co-Cr-Mo-C alloy. *J. Mater. Sci.* 17: 769-778.
- [6] J.R. Lane and N.J. Grant. 1957. Carbide reactions in high temperature alloys. *Trans. ASM.* 44: 113-137.
- [7] J.C. Zhao, M. Larsen, and V. Ravikumar. 2000. Phase precipitation and time-temperature-transformation diagram of Hastelloy X. *Mater. Sci. Eng. A.* 293:112-119.
- [8] Alfirano, S. Mineta, S. Namba, T. Yoneda, K. Ueda, and T. Narushima. 2011. Precipitates in as-cast and heat-treated ASTM F75 Co-Cr-Mo-C alloys containing Si and/or Mn. *Metall. Mater. Trans. A.* 42A: 1941-1949.
- [9] Alfirano, S. Mineta, S. Namba, T. Yoneda, K. Ueda, and T. Narushima. 2012. Precipitates in Biomedical Co-Cr-Mo-C-N-Si-Mn Alloys. *Metall. Mater. Trans. A.* 43A: 2125-2132.
- [10] Alfirano. 2015. Effect of Alloying Elements on Microstructure of Biomedical Co-Cr-Mo F75 Alloy. *Advanced Materials Research.* 1112: 421-424.
- [11] C. Montero, R. Juarez, and A. Rodriguez. 2012. Effect of fcc-hcp phase transformation produced by isothermal aging of a Co-27Cr-5Mo-0.05C alloy. *Metall. Mater. Trans. A.* 43A: 2125-2132.
- [12] Y.L. Dong, T.C. Chang, and G.L. Liu. 2003. Effect of Si contents on the growth behaviour of σ phase in SUS 309L stainless steels. *Script. Mater.* 49: 855-860.
- [13] S. Kurosu, N. Nomura, and A. Chiba. 2007. Microstructure and mechanical properties of Co-29Cr-6Mo alloy aged at 1023 K. *Mater. Trans.* 4: 1517-1522.